Articles

Development of a Pharmacophore Model for Histamine H_3 Receptor Antagonists, Using the Newly Developed Molecular Modeling Program SLATE

Iwan J. P. De Esch,*,§ James E. J. Mills,† Tim D. J. Perkins,† Giuseppe Romeo,‡,# Marcel Hoffmann,‡ Kerstin Wieland,‡ Rob Leurs,‡ Wiro M. P. B. Menge,‡ Paul H. J. Nederkoorn,‡ Philip M. Dean,§ and Henk Timmerman‡

De Novo Pharmaceuticals, St. Andrews House, 59 St. Andrews Street, CB2 3DD Cambridge, UK, Drug Design Group, Department of Pharmacology, University of Cambridge, Tennis Court Road, CB2 1QJ Cambridge, UK, and Leiden/Amsterdam Center for Drug Research (LACDR), Division of Medicinal Chemistry, Department of Pharmacology, Faculty of Chemistry, Vrije Universiteit, De Boelelaan 1083, 1081 HV Amsterdam, The Netherlands

Received November 6, 2000

New molecular modeling tools were developed to construct a qualitative pharmacophore model for histamine H_3 receptor antagonists. The program SLATE superposes ligands assuming optimum hydrogen bond geometry. One or two ligands are allowed to flex in the procedure, thereby enabling the determination of the bioactive conformation of flexible H_3 antagonists. In the derived model, four hydrogen-bonding site points and two hydrophobic pockets available for binding antagonists are revealed. The model results in a better understanding of the structure−activity relationships of H_3 antagonists. To validate the model, a series of new antagonists was synthesized. The compounds were designed to interact with all four hydrogen-bonding site points and the two hydrophobic pockets simultaneously. These ligands have high H_3 receptor affinity, thereby illustrating how the model can be used in the design of new classes of H_3 antagonists.

Introduction

Histamine mediates its actions via the stimulation of three distinct receptor subtypes, H_1, H_2, and H_3.[1] Selective antagonists of H_1 and H_2 receptors have been very successful in the treatment of allergic reactions and gastric ulcers, respectively, but the therapeutic use of H_3 receptor-related drugs has yet to be established. However, since the discovery of the H_3 receptor in 1983 by Arrang and co-workers,[2] considerable progress has been made in understanding the role of the H_3 receptor in (patho)physiology. The receptor controls neuronal synthesis of histamine[3] and, in addition, regulates the release of the neurotransmitter into the synaptic cleft.[4] Furthermore, it acts as a heteroreceptor at, e.g., serotoninergic, noradrenergic, cholinergic, dopaminergic, and peptidergic neurons.[5] H_3 receptors have been identified in peripheral tissues,[6] but the highest densities have been found in distinct areas of the central nervous system, especially in the areas that are associated with cognition.[7] Pharmacological studies have provided clear indications for the clinical use of selective H_3 ligands, and centrally active H_3 antagonists are considered potential therapeutic agents to treat neurological disorders such as obesity, epilepsy, sleeping disorders, and cognition and memory deficits.[8] Molecular modeling studies can give a fresh impetus to the design of new ligands. Recently, a pharmacophore model for histamine H_3 antagonists has been described.[9] The interaction of selected H_3 ligands with an aspartate residue of the receptor that is available for ligand binding was investigated. As two distinct lipophilic pockets available for ligand binding were revealed, the derived model explains the differences in structure−activity relationship (SAR) observed for the lipophilic tails of different classes of antagonists. However, detailed information about the relative location and shape of the distinct lipophilic pockets could not be obtained as the computational costs of the methods applied (a density functional approach using parallel supercomputers) prompted the truncation of the lipophilic tails of the antagonists to more manageable methyl groups. Furthermore, several classes of H_3 antagonists had to be omitted in the preliminary model as they lack a basic moiety that interacts with the aspartate residue.

Molecular similarity studies of the H_3 antagonists can be deceptive as several studies[10] have indicated that different classes of antagonists interact with different sets of (receptor) site points, i.e., indicating *partial* similarity.[11,12] Furthermore, modeling studies are seriously hampered by the flexibility of the H_3 ligands (vide infra).

To overcome the described problems, a new molecular modeling tool has been developed. The program SLATE superposes two flexible ligands assuming optimum hydrogen-bonding geometry. During the optimization, the ligands are represented by specific points used for

* Corresponding author. Tel: +44 1223 488810. Fax: +44 1223 488899. E-mail: Iwan.deEsch@denovopharma.com.
§ De Novo Pharmaceuticals.
† University of Cambridge.
‡ Vrije Universiteit.
# Present address: Dipartimento di Scienze Farmaceutiche, Università di Catania, v.le A. Doria 6, Catania, Italy.

10.1021/jm001109k CCC: $20.00
Published on Web 04/25/2001

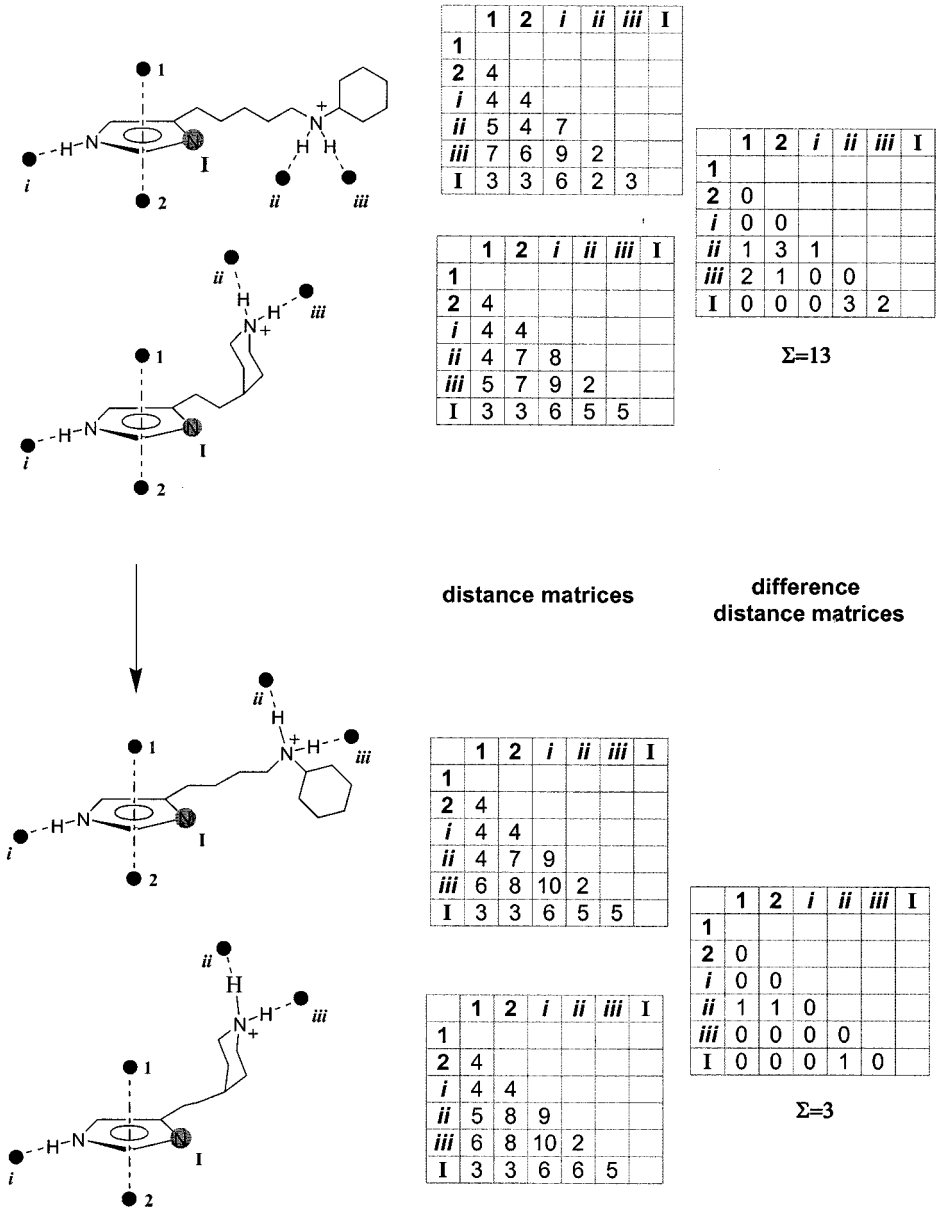

Figure 1. Schematic representation of the objective function calculated by the program SLATE. In this example, the points used for superposition are the ligand hydrogen-bonding acceptor atoms (I), the receptor hydrogen-bonding acceptor atoms (*i*, *ii*, and *iii*), and the two points on either side of the vector passing through aromatic centroids perpendicular to aromatic rings (1 and 2). The distances between these points are expressed in the distance matrix, and a difference distance matrix is calculated by subtraction of distance matrixes. The objective function in SLATE is the sum of the difference distance matrix elements. See text for details.

superposition, i.e., ligand hydrogen-bonding acceptor atoms, receptor hydrogen-bonding acceptor atoms (given by projecting ligand donor hydrogen atoms toward the optimum hydrogen-bonding position of the site), and aromatic rings. For each ligand, the 3D arrangement of the points used for superposition (the "pharmacophore") is expressed as a distance matrix (Figure 1). After every conformational change the difference distance matrix is calculated by subtraction of the distance matrixes. The objective function that is minimized by SLATE is the sum of the difference distance matrix elements, i.e., the score for the degree of similarity of the "pharmacophores" described by the two ligands. Simulated annealing is used for this minimization, which enables the rapid identification of good solutions, ideally the global minimum.[13] The procedure involves changing only the torsion angles and the relative ordering of corresponding points, thus being rapid enough to allow one or both ligands to flex. The resulting, optimized conformations are superposed (by rotation and transformation, while keeping the derived conformations fixed) using the MATFIT algorithm,[14] a so-called rigid fit procedure. Details and validation of SLATE have been described elsewhere.[15]

The Ligands. Different classes of H_3 antagonists are known; for a thorough review, the reader is referred to the literature.[16,17] One highly potent representative of the different classes is shown in Figure 2. The biological data stem from different pharmacological assays and are difficult to compare with respect to scale, error, and additional influences, restricting molecular modeling studies to more qualitative approaches. The most con-

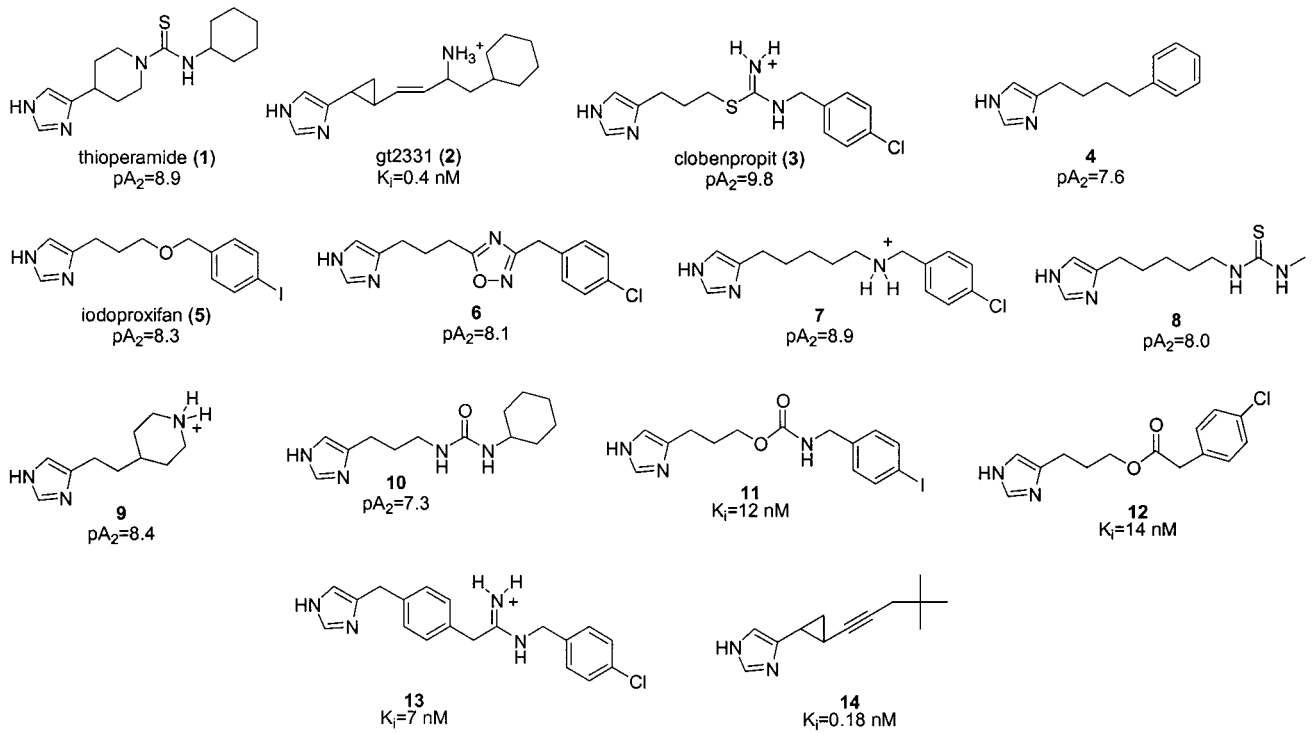

Figure 2. H_3 antagonists studied. The biological data are determined by evaluation of the influence of the compound on electrically evoked, cholinergic contractions of guinea pig intestine preparations (pA_2) or by evaluation of the influence of the compound on K^+-stimulated [^{3}H]-histamine release on rat cortex (pK_i).

served feature of H_3 ligands is the 4(5)-substituted imidazole ring that is essential for the activity. Whereas additional substituents on the imidazole ring lead to a dramatic reduction in activity, replacement of the imidazole by other functional groups results in compounds with no H_3 activity at all. This crucial role of the imidazole ring in most classes of H_3 antagonists indicates that at least this part of the ligands binds to the same receptor site and that this interaction is compulsory. It has to be noted that, very recently, new classes of H_3 antagonists have been described that lack an imidazole ring.[18] It has yet to be established whether these compounds interact at the same binding site of the H_3 receptor as the imidazole-containing ligands.

Several classes of antagonists shown in Figure 2 have an imidazole side chain that contains an N−H moiety which can interact with a hydrogen-bonding acceptor site (**1**, **2**, **3**, **7**, **8**, **9**, **10**, **11**, **13**). It has been shown that these basic pharmacophoric elements can interact with a hydrogen-bonding acceptor site point.[9,10] Attachment of a lipophilic residue ("tail") to this basic moiety can significantly influence the H_3 activity. For many classes of antagonists, cycloalkyl groups and (halogenated) benzyl groups lead to the most potent compounds within the given series.

Some classes of antagonists lack an N−H moiety in their imidazole side chain (**4**, **5**, **6**, **12**, **14**). Such compounds bind at the imidazole-binding site and a lipophilic pocket, obviously without interacting with the aforementioned hydrogen-bonding site point. The available data suggest that these ligands have a similar SAR with respect to the terminal lipophilic moiety, i.e., cycloalkyl or substituted benzyl groups leading to the most potent compounds. However, the SAR concerning the terminal lipophilic moiety throughout the different classes of H_3 antagonists is far from unambiguous, and many authors have suggested different binding sites for H_3 antagonists. For example, Stark and co-workers have proposed a different, unique binding mode for **3** and its derivatives, as substitution of the isothiourea group by halogenated benzyl groups leads to far more potent compounds than substitution with cycloalkyl groups.[19] Several authors have suggested an alternative binding mode for thioperamide (**1**) and its derivatives because these compounds also have a peculiar SAR concerning the lipophilic tail.[20−22] Vollinga et al. have described a class of antagonists (represented by **8**) lacking a significant influence of the type of lipophilic terminus on the activity.[23] None of these findings have been rationalized firmly.

Methods

The molecular coordinates of the ligands were constructed using MACROMODEL.[24] The basic nitrogen atoms in the side chain of the ligands were protonated except the nitrogen atoms of the urea, thiourea, and carbamate groups.[25,26] Since, at present, no indication exists about the bioactive tautomeric form of the imidazole moiety,[27] the N^t-H tautomer was arbitrarily selected for all investigated compounds. Aromatic regions were included in the matching procedure to ensure a tight superposition of the imidazole rings. The torsion angles of all single bonds were affected by the optimization procedure. Furthermore, the bonds of the isothiourea, thiourea, and amidine moieties were allowed to flip (180°) during the optimization to generate all possible configurations. For the structures containing a piperidine ring, all different ring conformers were generated and used as starting geometries. To this end, MACROMODEL[24] was used for molecular mechanics conformational analysis of the different possible ring structures (using the ring closure bond option). By

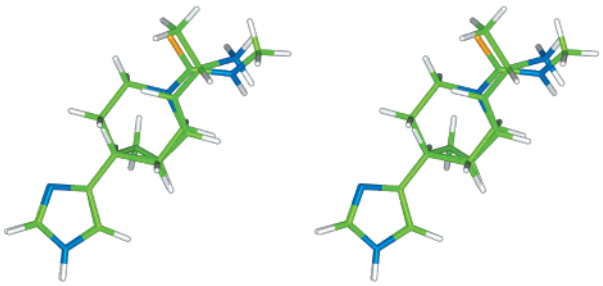

Figure 3. Construction of the pharmacophore by superimposing **1** and **2**, letting both compounds flex. The fit with the highest steric similarity is shown (stereoview). Carbon atoms are shown in green, oxygen atoms in red, nitrogen atoms in blue, sulfur atoms in yellow, and hydrogen atoms in white.

rotating all bonds through 360° with increments of 10°, a large number of conformations was generated. These conformations were energy optimized using the Amber force field[28] with the program BATCHMIN 2.7[24] in order to obtain low-energy conformations.

All trials using SLATE were run under the default annealing conditions.[15] Null correspondences were introduced according to literature procedures.[29,30] The so-called difference-distance matrix distance threshold parameter (see Mills and co-workers[15] for more details) was set equal to the high accuracy of 0.0001, to force exact superposition of pharmacophore points where possible. Fifty trials for each pair of molecules were run, and the trials in each set were ranked according to their steric similarity, calculated as the fraction of surface volume overlap by the program PLM.[31] Compounds **13** and **14** were fitted onto the pharmacophore using PSEUDO.[32] This program superposes a flexible ligand on a template by maximizing the overlap of the molecular skins. For each compound, 50 trials were run (using the default simulated annealing settings[15]). The fits with the best steric score were selected. For the superposed structures, the most likely positions of the complementary hydrogen-bonding atoms in the binding site were predicted using the program DOH.[30]

Construction of the Pharmacophore. Initially, the lipophilic tails of the antagonists used to construct the pharmacophore were truncated to methyl groups to facilitate steric evaluation of the fits and to circumvent the anticipated partial similarity problems that may accompany these substructures (vide supra). The approach of pairwise matching was applied, i.e., looking for one unique conformation of a reference ligand that is found in superposition trials with different ligands. Identical results were obtained irrespective of the particular ligand that was used as the reference structure. Here, the procedure will be described for thioperamide (**1**) as the reference structure. First, **1** (with the piperidine ring in the chair conformation) and GT2331 (**2**) were superposed by running 50 trials of SLATE, allowing both compounds to flex. The fit with the best steric score is shown in Figure 3. In total, six different conformations of **1**, called set I, were found to match different conformations of **2**. In a similar experiment, thioperamide (**1**) and clobenpropit (**3**) were superposed, allowing both ligands to flex. Many different conformations of the ligands within this set II were found. However, comparison of the conformations of thioperamide (**1**) in set I and set II revealed that only

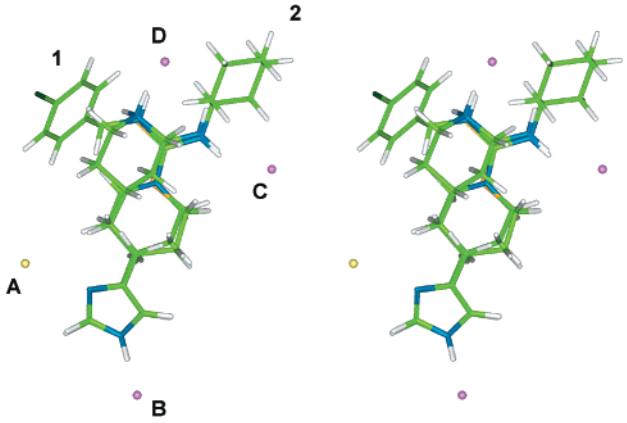

Figure 4. Superposition of ligands **1**, **3**, and **9** (stereoview) illustrates the position of the four hydrogen-bonding site points (A−D) and two lipophilic pockets (1 and 2) and gives an indication about the steric requirements of the derived pharmacophore. The most likely positions of the receptor site points were calculated using the program DOH.[31] Acceptor site points are shown in magenta and donor site points in yellow.

one conformation was found in both sets. Furthermore, this unique conformation of thioperamide was found in the superpositions that had the highest steric similarity score in both sets I (Figure 3) and II (not shown). Therefore, this conformation of thioperamide, and the corresponding conformations of **2** and **3**, were accepted as the bioactive conformations. A unique pharmacophore could only be found when the piperidine ring of **1** was in the chair conformation. When the piperidine ring was (fixed) in a different conformation, no identical conformations of the reference ligand **1** in the different sets could be found.

As can be seen in Figure 3, the methyl groups (that substitute the lipophilic tails) of the antagonists **1** and **2** have a different position and orientation, indicating that this procedure finds two lipophilic pockets available for antagonist binding, thereby validating earlier findings.[9] Figure 3 also illustrates that it is not necessary to force the basic nitrogen atoms of the ligands to occupy the same position in space. A certain degree of positional freedom for these substructures is allowed to obtain an optimal position to interact with the complementary hydrogen-bonding site points, hence taking into account the directionality of the intermolecular hydrogen bond.

The lipophilic tail of **1** and **2**, a cyclohexyl group in both cases, was added using the program MacroModel. This substructure was energy-optimized using the Amber force field[28] while the positions of all other atoms of the template were frozen. The relative position of the lipophilic tail of clobenpropit (**3**), a 4-Cl-benzyl group, was determined using SLATE. Again, the approach of pairwise matching was used. The complete flexible antagonists **4**, **5**, and **6**, were matched with clobenpropit **3** that was fixed in the bioactive conformation (as described in a previous subsection) except for the lipophilic tail and the bonds of the isothiourea group, which were allowed to flip 180°. Comparing the three sets as described before revealed the unique relative position of the lipophilic tails.

The superposed structures describe the relative position and orientation of the imidazole moieties, the basic groups in the imidazole side chain, and the lipophilic tails of these ligands (see Figure 4). Subsequent ligands

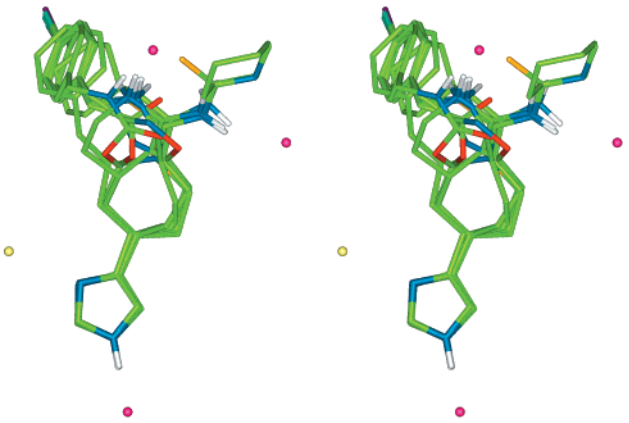

Figure 5. Superposition of ligands **1**−**12** (stereoview). Hydrogen atoms attached to carbon atoms are omitted.

were fitted onto this pharmacophore. In all cases, the fit with the highest steric score was selected. This procedure reveals four hydrogen-bonding site points. Obviously, the two site points that can interact with the basic moiety in the imidazole side chains of the H_3 ligands introduce another cause for partial similarity. It has to be noted that the position of both side points was confirmed by using different combinations of reference and subsequent structures and using SLATE to determine the bioactive conformations by allowing all structures to flex.

Results and Discussion

The binding site for histamine H_3 receptor antagonists can be described by four hydrogen-bonding site points and two lipophilic pockets. The relative orientation of these features is shown in Figure 4 by superposition of ligands **1**, **3**, and **9**, which also gives an excellent illustration of the steric requirements of the derived pharmacophore. The imidazole moiety of the ligands interacts with site points A and B. Basic nitrogen atoms of the imidazole side chain of the ligands can interact with site points C and/or D. Only clobenpropit (**3**) is able to interact with all four hydrogen-bonding site points simultaneously. This might explain the high potency of this antagonist.

Figure 5 shows the ligands **1**−**12** which were superposed using SLATE. Pocket 1 is occupied by antagonists **2**, **3**, **4**, **5**, **6**, **7**, **10**, **11**, and **12**. These antagonists have cycloalkyl- and (substituted-) benzyl- groups. The hydrophobic region is easily accessible, and (as is apparent from the SAR) with the proper lipophilic tail, a high increase in affinity is obtained. The lipophilic tails of **1** and **8** interact with hydrophobic pocket 2 (Figure 5). The entrance to this pocket seems to be rather narrow, being enclosed by the two site points C and D. The thiourea moieties of ligands **1** and **8** are only partly overlapping, so the orientation, and hence the SAR, of the lipophilic tails are different.

Detailed information about the shape of pocket 2 was obtained by incorporation of the results of a QSAR study.[20] It was reported that substitution of the cyclohexyl group of **1** by substituted benzyl groups leads to ligands with reduced activity. The position of the substituent on the benzyl group had a peculiar effect on the activity, with ortho substituents being more favorable for H_3 antagonistic activity than para substituents.

Table 1. Histamine H_3 Antagonistic Activity and Calculated Torsion Angle φ of Two Selected Thioperamide Derivatives as Published in a QSAR Study by Windhorst and Co-workers[20]

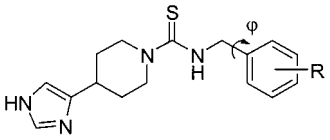

cmpd	R	pA_2 (±sem)	φ, deg
15	2-Cl	8.21 (0.09)	−168.5
16	4-Cl	7.21 (0.08)	−122.2

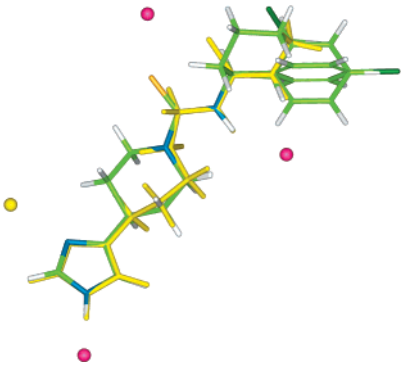

Figure 6. Detailed description of the shape of pocket 2 by superposing **1**, **8** (yellow), **15**, and **16**. See text for details.

In this QSAR study, using 15 thioperamide derivatives, it was revealed that the latter effect was caused by the unique character of the piperidine-1-carbothioic acid amide moiety. A correlation was found between the activity of the different analogues and the torsion angle φ of these compounds (illustrated in Table 1).

Incorporation into our pharmacophore model of two of these compounds (**15** and **16**), frozen in the conformation predicted by Windhorst et al,[20] illustrates that the 2-Cl benzyl group of **15** uses the same plane in 3D space as the methyl group of **8** and the cyclohexyl group of **1** (Figure 6). However, the 4-Cl benzyl group of the less active compound **16** is twisted out of this plane. Thus, the more active ortho-substituted derivative is in better steric agreement with the pharmacophore for H_3 antagonists, as was already implied by the aforementioned QSAR study.

Surprisingly, compound **13** could not be fitted into the pharmacophore using SLATE. Using PSEUDO under the default conditions,[32] a conformation of ligand **13** was derived (Figure 7) in which the amidine moiety does not interact with the hydrogen-bonding acceptor site points C or D, explaining why SLATE did not find this conformation. No data for the role of the amidine group are available, but the theoretical considerations presented here indicate that this group is not involved in hydrogen-bonding interaction with the receptor. The program PSEUDO was also used to fit compound **14**. No thorough structural variations of the lipophilic tail of this antagonist (i.e., the *tert*-butyl group) have been reported. Therefore, no experimental data are available that could indicate whether the compound interacts with pocket 1 or pocket 2. The program PSEUDO indicates that the *tert*-butyl group of **14** occupies pocket 2 (Figure 8). One of the methyl groups of this moiety is positioned just above the center of the cyclohexyl ring

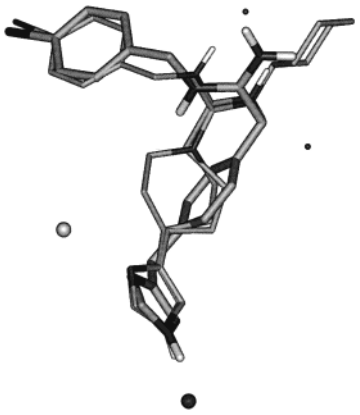

Figure 7. Superposition of **1**, **3**, and **13** (the latter in bold). Compound **13** cannot interact with site points C or D. Hydrogen atoms attached to carbon atoms are omitted.

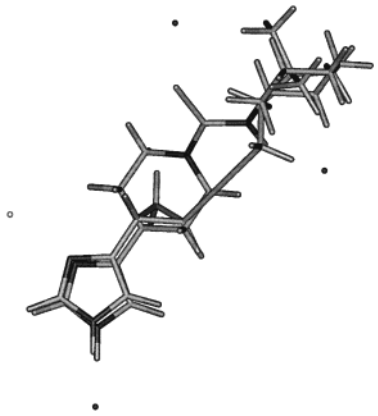

Figure 8. Superposition of **1** and **14**.

of thioperamide. This is in perfect agreement with recently published data in which it was shown that replacement of the cyclohexyl ring of thioperamide (**1**) by an adamantyl group results in a slightly more potent H_3 antagonist.[33] The chiral cyclopropyl units of **2** and **14** occupy exactly the same position in 3D space as might be expected when considering the stereospecificity of the H_3 receptor.

Validation of the Pharmacophore. Design and Synthesis. To validate the presence of two hydrophobic pockets available for H_3 antagonist binding, a small series of compounds was designed and synthesized, and the affinity of the ligands for the H_3 receptor was determined. For this study, clobenpropit (**3**) was an ideal lead compound, as a (substitutable) hydrogen atom of the isothiourea moiety is pointing directly toward the second hydrophobic pocket. On the basis of the pharmacophore model, the receptor can accommodate a cyclohexyl group in this position, as is illustrated in Figure 9 by the superposition of clobenpropit (**3**) and thioperamide (**1**). In addition to the interaction with two hydrophobic pockets, the compounds have interaction with all four hydrogen-bonding site points.

The ligands **22**−**25** were synthesized according to Scheme 1. Intermediate 4-(3-bromo-propyl)-1*H*-imidazole hydrobromide (**17**) was treated with thiourea compounds (**18**−**21**) to yield the target ligands (**22**−**25**). The thiourea compounds (**18**−**21**) were prepared from commercially available isothiocyanates and the corresponding amines.

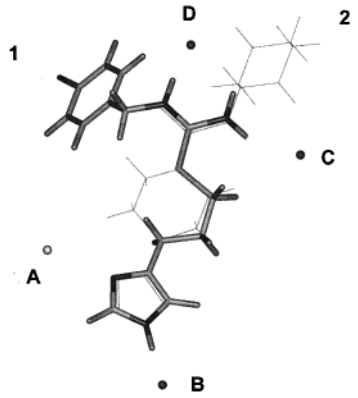

Figure 9. Superposition of thioperamide (**1**) (in faint) and clobenpropit (**3**).

Scheme 1[a]

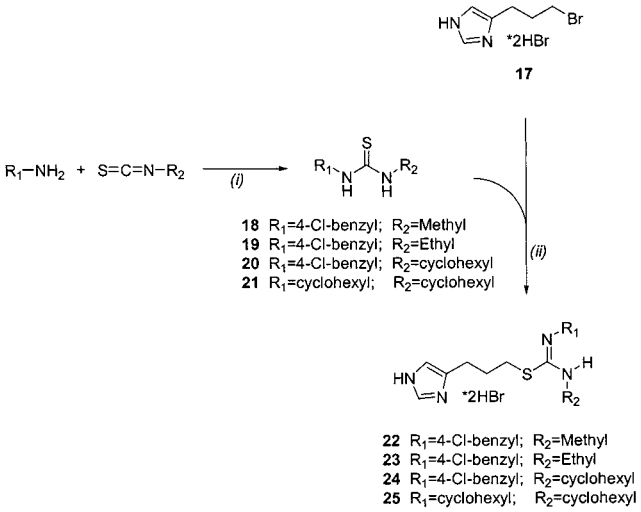

[a] (*i*) DCM; (*ii*) ethanol, Δ.

Scheme 2[a]

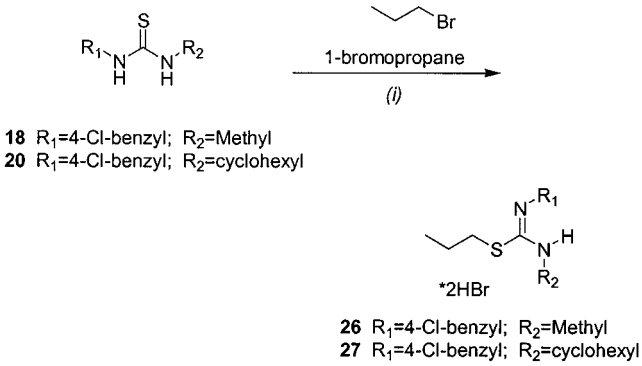

[a] (*i*) ethanol, HBr, Δ.

To investigate the necessity of the imidazole moiety, the two nonimidazole compounds **26** and **27** were synthesized, via an analogous route (Scheme 2).

Pharmacology. The affinity for the histamine H_3 receptor was determined by displacement of the radioligand [^{3}H] N^{α}-methylhistamine using membrane homogenates of rat cerebral cortex.

Results

Substitution of the isothiourea group of clobenpropit by a methyl or ethyl group results in a significant decrease of H_3 affinity (Table 2). However, with the

Table 2. Histamine H_3 Receptor Binding Affinity of the Designed Compounds

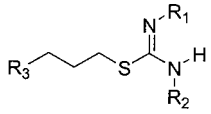

cmpd	name	R_1	R_2	R_3	pK_i
3	clobenpropit	4-Cl-benzyl	H	4(5)-imidazolyl	9.6 ± 0.1
22	VUF 5224	4-Cl-benzyl	methyl	4(5)-imidazolyl	8.5 ± 0.1
23	VUF 5225	4-Cl-benzyl	ethyl	4(5)-imidazolyl	8.1 ± 0.1
24	VUF 5228	4-Cl-benzyl	*cyclo*-hexyl	4(5)-imidazolyl	9.3 ± 0.2
25	VUF 5642	*cyclo*-hexyl	*cyclo*-hexyl	4(5)-imidazolyl	7.9 ± 0.1
26	VUF 5649	4-Cl-benzyl	methyl	H	<4
27	VUF 5650	4-Cl-benzyl	*cyclo*-hexyl	H	5.3 ± 0.07

cyclohexyl-substituted compound **24**, the high H_3 affinity (pK_i = 9.3 ± 0.2) is regained. Attachment of two cyclohexyl groups to the isothiourea (compound **25**) leads to a significant decrease in activity (pK_i = 7.9 ± 0.1).

This series of compounds reveals that the H_3 receptor can accommodate antagonists which have two lipophilic moieties in their imidazole side chain, thereby validating the pharmacophore model. It is also shown that H_3 affinity is influenced not only by the putative hydrophobic interaction of two isothiourea substituents and the two different pockets of the receptor (compare **22** and **24**). Additional factors (e.g., electronic effects) have an influence on the interaction of the ligands with the receptor (compare **22**, **24**, and **25**, noting that the electron-releasing substituents on the isothiourea group may reduce the interaction of the isothiourea moiety and the two hydrogen-bonding acceptor site points). A thorough quantitative structure−activity relationship study is needed to unravel the precise contribution of the distinct physical properties of the isothiourea substituents on the H_3 affinity.

The deletion of the imidazole heterocycle proves to be disastrous for H_3 affinity (Table 2). These results again illustrate the major influence of the imidazole nucleus on the H_3 receptor affinity of ligands at this binding site.[10] Interestingly, replacement of the methyl group of **26** by a cyclohexyl group, leading to **27**, results in a better H_3 ligand. A similar improvement can be seen when comparing the imidazole-containing compounds **22** and **24**. However, it has to be noted that straightforward comparison of non-imidazole ligands **26** and **27** and the imidazole-containing compounds **22** and **24** is ambiguous as the non-imidazole compounds might interact with a different binding site of the H_3 receptor.

Conclusions

Using newly developed molecular modeling techniques, a pharmacophore model for histamine H_3 antagonists has been derived. The binding site of the histamine H_3 receptor is characterized by four hydrogen-bonding site points and two lipophilic pockets. Although qualitative by necessity, this study gives an explanation of the observed differences in SAR found for H_3 receptor antagonists. The new model has been used to design new antagonists that interact with all four hydrogen-bonding site points and the two distinct lipophilic pockets simultaneously. These results illustrate that the model can be used to design novel classes of antagonists.

Experimental Section

Chemistry. General Procedure. ^{1}H and ^{13}C NMR spectra were recorded on a Bruker AC-200 spectrometer (unless indicated otherwise) with tetramethylsilane as an internal standard. Melting points were determined on an Electrothermal IA9200 apparatus and are uncorrected. Solvents were purified and dried by standard procedures. 4-(3-Bromo-propyl)-1*H*-imidazole hydrobromide (**17**) was prepared according to literature procedure.[34,35]

***N*-Methyl-*N*′-(4-chlorobenzyl)thiourea (18).** To a solution of methyl isothiocyanate (2.19 g, 30.0 mmol) in anhydrous diethyl ether (25 mL) was added dropwise a solution of 4-chlorobenzylamine (4.25 g, 30.0 mmol) in anhydrous diethyl ether (25 mL). After vigorously stirring the suspension for 2 h, the precipitated product was collected by filtration, washed with anhydrous diethyl ether (20 mL), and dried. A white solid was isolated (5.65 g, 88%) which was pure by TLC (eluent $CHCl_3$) and was used without further purification. An analytical sample was recrystallized from toluene. Mp: 109.5−110.5 °C. ^{1}H NMR ($CDCl_3$): δ 2.96 (d, J = 5.3 Hz, 3H), 4.67 (d, J = 6.0 Hz, 2H), 6.18 (bs, 2H), 7.18−7.24 (m, 4H).

***N*-(4-Chlorobenzyl)-*N*′-ethylthiourea (19).** Analogous to the preparation of **18**, using ethyl isothiocyanate. Recrystallized from toluene, yield 90%. Mp: 100−101 °C. ^{1}H NMR ($CDCl_3$): δ 1.19 (t, J = 6.7 Hz, 3H), 3.28−3.48 (m, 2H), 4.65 (d, J = 6.0 Hz, 2H), 5.95 (bs, 1H), 7.18−7.24 (m, 4H).

***N*-(4-Chlorobenzyl)-*N*′-cyclohexylthiourea (20).** Analogous to the preparation of **18**, using cyclohexyl isothiocyanate. Recrystallized from toluene, yield 76%. Mp: 115.5−116 °C. ^{1}H NMR ($CDCl_3$): δ 0.95−2.10 (m, 10H), 3.80 (m, 1H), 4.58 (d, J = 6.0 Hz, 2H), 5.90 (bs, 1H), 6.28 (bs, 1H), 7.10−7.30 (m, 4H).

***N*,*N*′-Biscyclohexylthiourea (21).** Analogous to the preparation of **18**, using cyclohexylamine and cyclohexyl isothiocyanate. Recrystallized from toluene, yield 24%. Mp: 180−182 °C. ^{1}H NMR ($CDCl_3$): δ 1.02−2.10 (m, 20H), 3.80 (m, 2H), 5.64 (bs, 2H).

***N*-(4-Chlorobenzyl)-*S*-[3-(4(5)-imidazolyl)propyl]-*N*′-methyl-isothiourea Dihydrobromide (22).** A solution of **18** (2.70 g, 10.0 mmol) and 4-(3-Bromo-propyl)-1*H*-imidazole hydrobromide (**17**) in ethanol (25 mL) was refluxed for 48 h. The reaction mixture was concentrated in vacuo, and the residue was purified by column chromatography (acetate/methanol, 3/1, v/v). The product was precipitated in acetone to give a white solid (0.85 g, 18%). Mp: 163.0−164.0 °C. ^{1}H NMR (DMSO-d_6): δ 1.80−2.08 (m, 2H), 2.73 (t, J = 7.5 Hz, 2H), 3.05 (s, 3H), 3.22−3.50 (m, 3.8 H), 4.64 (s, 2H), 7.30−7.52 (m, 5H), 9.04 (s, 1H). Anal. ($C_{15}H_{21}Br_2ClN_4S$) C, H, N.

***N*-(4-Chlorobenzyl)-*N*′-ethyl-*S*-[3-(4(5)-imidazolyl)propyl]isothiourea Dihydrobromide (23).** Analogous to the preparation of **22**, using **19**. The product was isolated as an oil (25%). ^{1}H NMR (DMSO-d_6): δ 1.20 (t, J = 7.3 Hz, 3H), 1.75−2.03 (m, 2H), 2.71 (t, J = 7.5 Hz, 2H), 3.10−3.65 (m, 5.8 H), 4.66 (s, 2H), 7.20−7.58 (m, 5H), 8.98 (s, 1H). Anal. ($C_{16}H_{23}Br_2ClN_4S$) C, H, N.

***N*-(4-Chlorobenzyl)-*N*′-cyclohexyl-*S*-[3-(4(5)-imidazolyl)-propyl]isothiourea Dihydrobromide (24).** Analogous to

the preparation of **22**, using **20**. After purification by column chromatography and evaporation of a uniform fraction, the semisolid residue was suspended in dry diethyl ether and stirred until complete precipitation. The very hygroscopic material was filtered and dried. Yield: 22%. Mp: 127.0−130.0 °C. ^{1}H NMR (DMSO-d_6): δ 1.00−2.08 (m, 12H), 2.67 (t, J = 7.5 Hz, 2H), 3.31 (t, J = 7.2 Hz, 2H), 3.79 (m, 1H), 4.68 (s, 2H), 7.29−7.51 (m, 5H), 8.81 (s, 1H). Anal. ($C_{20}H_{29}Br_2ClN_4S$) C, H, N.

***N,N′*-Biscyclohexyl-*S*-[3-(4(5)-imidazolyl)propyl]isothiourea Dihydrobromide (25).** Analogous to the preparation of **22**, using **21**. The product was isolated as a white solid (18%). ^{1}H NMR (DMSO-d_6): δ 1.00−2.08 (m, 22H), 2.74 (t, J = 7.5 Hz, 2H), 3.32 (t, J = 7.0 Hz, 2H), 3.63−3.90 (m, 2H), 7.47 (s, 1H), 8.95 (s, 1H). Anal. ($C_{19}H_{34}Br_2N_4S$) C, N; H: calcd, 6.71; found, 5.73.

***N*-(4-Chlorobenzyl)-*N′*-methyl-*S*-propyl]isothiourea Hydrobromide (26).** Analogous to the preparation of **22**, using **18** and 1-bromopropane. The crude product was purified by chromatography ($CHCl_3$/methanol, 95/5, v/v). A white product was isolated (43%). Mp: 107.5−108.5 °C. ^{1}H NMR ($CDCl_3$): δ 0.96 (t, J = 7.5 Hz, 3H), 1.50−1.75 (m, 2H), 3.04 (s,3H), 3.47 (t, J = 6.0 Hz, 2H), 4.59 (s, 2H), 7.60 (br s, 1H), 7.14−7.38 (m, 4H), 9.70 (bs, 1H). Anal. ($C_{12}H_{18}BrClN_2S$) C, H, N.

***N*-(4-Chlorobenzyl)-*N′*-cyclohexyl-*S*-propyl]isothiourea Hydrobromide (27).** Analogous to the preparation of **26**, using **20**. A white solid was obtained (43%). Mp: 146.0−147.0 °C. ^{1}H NMR ($CDCl_3$): δ 0.94 (t, J = 7.34 Hz, 3H), 1.03−1.93 (m, 10H), 1.51−1.68 (m, 2H), 3.11 (t, J = 5.34 Hz, 2H), 3.64−3.88 (m, 1H), 4.67 (s, 2H), 6.28 (bs, 1H), 7.12−7.41 (m, 4H). Anal. ($C_{17}H_{26}BrClN_2S$) C, H, N.

Pharmacology. The histamine H_3 receptor affinity was determined on rat cortical membranes with [^{3}H]-N^α-methylhistamine (81.9 Ci/mmol, NEN life science products, Brussels, Belgium) according to the method of West et al.[36] with modifications. Briefly, animals were killed by decapitation, and the cerebral cortex rapidly removed. Rat cortices were homogenized in 15 volumes (wt/vol.) of ice-cold Tris/HCl buffer (50 mM Tris/HCl; 5 mM $MgCl_2$, 145 mM NaCl; pH 7.4 at 4 °C) using an Ultra-Turrax homogenizer (8 s) and a glass-Teflon homogenizer (four strokes up and down) subsequently. All subsequent steps were carried out at 0−4 °C. The homogenate was centrifuged at 800*g* for 10 min. The pellets were discarded, and the supernatant was centrifuged for 20 min at 40000*g*. The resulting pellet was resuspended, and the last centrifugation step was repeated. The pellet was resuspended in 1.5 volume (wt/vol.) Tris/HCl buffer to give a final concentration of ~300 μg/100 μL and stored in aliquots at −80 °C. Protein concentration was determined using Biorad protein assay (Bio-Rad laboratories GmbH, Munich, Germany). Competition binding experiments were carried out in polypropylene tubes in a total volume of 400 μL of 50 mM Na^+ phosphate buffer pH 7.4 at 37 °C, containing 30 μg of protein, 1nM of [^{3}H]-N^α methylhistamine, and 0.1 to 10 000 nM of the compound to be tested. Samples were incubated for 40 min at 25 °C. The incubation was started by the addition of 100 μL of membranes (30 μg) and terminated by rapid filtration through polyethyleneimine (0.3 wt %/vol.) pretreated Whatman GF/C filters using a Brandel filtration apparatus. The filters were washed twice with 3 mL of ice-cold Tris/HCl buffer (50 mM Tris/HCl; 5 mM $MgCl_2$, 145 mM NaCl; pH 7.4 at 4 °C). The radioactivity retained on the filters was measured using liquid scintillation counting. Competition isotherms were analyzed with the GraphPad Prism software (GraphPad, Intuitive Software for Science, San Diego, CA). K_i values were determined with the equation $K_i = IC_{50}/(1 + ([\text{ligand}]/K_d))$.

Acknowledgment. This research was in part (I.D.E.) supported by the Dutch Technology Foundation (STW).

References

(1) Leurs, R.; Smit, M. J.; Timmerman, H. Molecular pharmacological aspects of histamine receptors. *Pharmacol. Ther.* **1995**, *66*, 413−463.

(2) Arrang, J. M.; Garbarg, M.; Schwartz, J.-C. Auto-inhibition of brain histamine release mediated by a novel class (H_3) of histamine receptor. *Nature* **1983**, *302*, 832−837.

(3) Arrang, J.-M.; Garbarg, M.; Schwartz, J.-C. Autoinhibition of histamine synthesis mediated by presynaptic H_3-receptors. *Neuroscience* **1987**, *13*, 149−157.

(4) Arrang, J.-M.; Garbarg, M.; Schwartz, J.-C. Autoregulation of histamine release in brain by presynaptic H_3-receptors. *Neuroscience* **1985**, *15*, 553−562.

(5) Schlicker, E.; Kathmann, M. Modulation of in vitro neurotransmission in the CNS and in the retina via H_3 heteroreceptors. In *The histamine H3 receptor; a target for new drugs*, 1st ed.; Leurs, R., Timmerman, H., Eds.; Elsevier Science B. V.: Amsterdam, 1998; pp 13−26.

(6) Bartaccini, G.; Coruzzi, G.; Poli, E. Functional role of histamine H_3 receptors in peripheral tissues. In *The histamine H3 receptor; a target for new drugs*, 1st ed.; Leurs, R., Timmerman, H., Eds.; Elsevier Science B. V.: Amsterdam, 1998; pp 59−112.

(7) Arrang, J.-M.; Garbarg, M.; Lancelot, J.-C.; Lecomte, J.-M.; Pollard, H.; Robba, M.; Schunack, W.; Schwartz. J.-C. Highly potent and selective ligands for histamine H_3-receptors. *Nature* **1987**, *327*, 117−123.

(8) Leurs, R.; Blandina, P.; Tedford, C.; Timmerman, H. Therapeutic potential of histamine H_3 receptor agonists and antagonists. *Trends Pharmacol. Sci.* **1998**, *19*, 177−183.

(9) De Esch, I. J. P.; Timmerman, H.; Menge, W. M. P. B.; Nederkoorn, P. H. J. A qualitative model for the histamine H_3 receptor explaining agonistic and antagonistic activity simultaneously. *Arch. Pharm. Pharm. Med. Chem.* **2000**, *333*, 254−260.

(10) De Esch, I. J. P.; Gaffar, A.; Menge, W. M. P. B.; Timmerman, H. Synthesis and histamine H_3 receptor activity of 4-(*n*-alkyl)-1*H*-imidazoles and 4-(*ω*-phenylalkyl)-1*H*-imidazoles. *Bioorg. Med. Chem.* **1999**, *7*, 3003−3008.

(11) Mattos, C.; Ringe, D. Multiple binding modes. In *3D QSAR in drug design: theory, methods and applications*; Kubinyi, H., Ed.; Escom: Leiden, 1993; pp 226−254.

(12) Perkins, T. D. J.; Mills, J. E. J.; Dean, P. M. Molecular partial similarity using surface-volume comparisons. In *Computer-assisted lead finding and optimization*; van de Waterbeemd, H., Testa, B., Folkers, G., Eds.; VCH: Weinheim, 1997; pp 421−432.

(13) Barakat, M. T.; Dean, P. M. Molecular structure matching by simulated annealing. *J. Comput.-Aided Mol. Des.* **1990**, *4*, 295−316.

(14) McLachlan, A. D. Gene duplication in the structural evolution of chymotrypsin. *J. Mol. Biol.* **1979**, *128*, 49−79.

(15) Mills, J. E. J.; De Esch, I. J. P.; Perkins, T. D. J.; Dean, P. M. SLATE: a method for the superposition of flexible ligands. *J. Comput.-Aided. Mol. Des.* **2001**, *15*, 81−96.

(16) Leurs, R.; Vollinga, R. C.; Timmerman, H. The medicinal chemistry and therapeutic potentials of ligands of the histamine H_3-receptor. *Prog. Drug Res.* **1995**, *45*, 107−165.

(17) Lipp, R.; Stark, H.; Schunack, W. Pharmacochemistry of H_3 Receptors: The histamine receptor. In *Receptor Biochemistry and Methodology*; Schwartz, J.-C., Haas, H. L., Eds.; Wiley-Liss Inc.: New York, 1992; Vol. 16; pp 57−72.

(18) Ganellin, C. R.; Leurquin, F.; Piripitsi, A.; Arrang, J.-M.; Garbarg, M.; Ligneau, X.; Schunack, W.; Schwartz, J.-C. Synthesis of potent non-imidazole histamine H_3-receptor antagonists. *Arch. Pharm. Pharm. Med. Chem.* **1998**, *331*, 395−404.

(19) Stark, H.; Purand, K.; Ligneau, X.; Rouleau, A.; Arrang, J.-M.; Garbarg, M.; Schwartz, J.-C.; Schunack.; W. Novel carbamates as potent histamine H_3 receptor antagonists with high in vitro and oral in vivo activity. *J. Med. Chem.* **1996**, *39*, 1157−1163.

(20) Windhorst, A. D.; Timmerman, H.; Worthington, E. A.; Bijloo, G. J.; Nederkoorn, P. H. J.; Menge, W. M. P. B.; Leurs, R.; Herscheid, J. D. M. Characterization of the binding site of the histamine H_3 receptor. 3. Synthesis, in vitro pharmacology and QSAR of a series of monosubstituted benzyl analogues of thioperamide. *J. Med. Chem.* **2000**, *43*, 1754−1761.

(21) Ganellin, C. R.; Hosseini, S. K.; Khalaf, Y. S.; Tertiuk, W.; Arrang, H.-M.; Garbarg, M.; Ligneau, X. Schwartz, J.-C. Design of potent non-thiourea H_3-receptor histamine antagonists. *J. Med. Chem.* **1995**, *38*, 3342−3350.

(22) Plazzi, P. V.; Bordi, F.; Mor, M.; Silva, C.; Morini, G.; Caretta, A.; Barocelli, E.; Vitali, T. Heteroarylaminoethyl and heteroarylthioethyl imidazoles. Synthesis and H_3-receptor affinity. *Eur. J. Med. Chem.* **1995**, *30*, 881−889.

(23) Vollinga, R. C.; Menge, W. M. P. B.; Leurs, R.; Timmerman, H. New analogs of burimamide as potent and selective histamine H_3 receptor antagonists, the effect of chain length variation of the alkyl spacer and modifications of the N-thiourea substituent. *J. Med. Chem.* **1995**, *38*, 2244−2250.

(24) Mohamadi, F.; Richards, N. G. J.; Guida, W. C.; Liskamp, R.; Lipton, M.; Caufield, C.; Chang, G.; Hendrickson, T.; Still, W. C. MacroModel -An integrated software system for modeling organic and bioorganic molecules using molecular mechanics. *J. Comput. Chem*. **1990**, *11*, 440−467.
(25) Smith, S. E.; Rawlins, M. D. *Variability in Human Drug Response*; Butterworth: London, 1973; pp 154−165.
(26) Mor, M.; Bordi, F.; Silva, C.; Rivara, S.; Crivori, P.; Vincenzo Plazzi, P.; Ballabeni, V.; Caretta, A.; Barocelli, E.; Imicciatore, M.; Carrupt, P.-A.; Testa, B. H_3-Receptor antagonists: synthesis and structure−activity relationships of para- and meta-substituted 4(5)-phenyl-2-[[2-[4(5)-imidazolyl]ethyl]thio]imidazoles. *J. Med. Chem*. **1997**, *40*, 2571−2578.
(27) De Esch, I. J. P.; Nederkoorn, P. H. J.; Timmerman, H. Molecular modelling studies of histamine H_3 receptor ligands. In *The histamine H3 receptor; a target for new drugs*, 1st ed.; Leurs, R., Timmerman, H., Eds.; Elsevier Science B. V.: Amsterdam, 1998; pp 59−112.
(28) Weiner, S. J.; Kollman, P. A.; Nguyen, D. T.; Case, D. A. An all atom force field for simulations of proteins and nucleic acids. *J. Comput. Chem*. **1986**, *7*, 230−252.
(29) Barakat, M. T.; Dean, P. M. Molecular structure matching by simulated annealing. III. The incorporation of null correspondences into the matching problem. *J. Comput.-Aided Mol. Des.* **1991**, *5*, 107−117.
(30) Mills, J. E. J.; Perkins, T. D. J.; Dean, P. M. An automated method for predicting the positions of hydrogen-bonding atoms in binding sites. *J. Comput.-Aided Mol. Des.* **1997**, *11*, 229−242.
(31) Perkins, T. D. J.; Mills, J. E. J.; Dean, P. M. Molecular surface-volume and property matching to superpose flexible and dissimilar molecules. *J. Comput.-Aided Mol. Des.* **1995**, *9*, 479−490.
(32) The program PSEUDO is like the program in ref 12, but conformational flexibility is allowed during the optimization.
(33) Goto, T.; Sakashita, H.; Murakami, K.; Sugiura, M.; Kondo, T.; Fukaya, C. Novel histamine H_3 receptor antagonists: synthesis and evaluation of formamidine and S-methylisothiourea derivatives. *Chem. Pharm. Bull.* **1997**, *45*, 305−311.
(34) Kivits, G.; Hora, J. *J. Heterocycl. Chem*. **1975**, *12*, 577.
(35) Bloemhoff, W.; Kerling, K. *Recueil Trav. Chim. Pays Bas* **1970**, *89*, 1181.
(36) West, R. E. J.; Zweig, A.; Shih, N. Y.; Siegel, M. I.; Egan, R. W.; Clark, M. A. Identification of two receptor subtypes. *Mol. Pharmacol.* **1990**, *38*, 610−613.

JM001109K